frontiers | Frontiers in Energy Research

METHODS
published: 08 April 2022
doi: 10.3389/fenrg.2022.856943

A Thermogravimetric Temperature-Programmed Thermal Redox Protocol for Rapid Screening of Metal Oxides for Solar Thermochemical Hydrogen Production

Michael D. Sanders[1], *Anyka M. Bergeson-Keller*[1], *Eric N. Coker*[2] *and Ryan P. O'Hayre*[1]*

[1]Colorado School of Mines, Department of Metallurgy and Materials Engineering, Colorado Center for Advanced Ceramics, Golden, CO, United States, [2]Sandia National Laboratories, Albuquerque, NM, United States

As combinatorial and computational methods accelerate the identification of potentially suitable thermochemically-active oxides for use in solar thermochemical hydrogen production (STCH), the onus shifts to quickly evaluating predicted performance. Traditionally, this has required an experimental setup capable of directly carrying out a two-stage thermochemical water-splitting process. But this can be a difficult endeavor, as most off-the-shelf equipment cannot adequately deal simultaneously with the high temperatures, varying oxygen partial pressures, and high H_2O partial pressures required; achieving sufficient temporal sensitivity to accurately quantify the kinetics is also a major challenge. However, as proposed here, a less complicated experiment can be used as a first screening for thermochemical water splitting potential. Temperature-Programmed Thermal Redox (TPTR) using thermogravimetry evaluates the thermal reduction behavior of materials. This technique does not require water splitting or CO_2-splitting analogs but can nonetheless predict water-splitting performance. Three figures of merit are obtained from the TPTR experiment: reduction onset temperature, extent of reduction, and extent of recovery upon reoxidation. These metrics can collectively be used to determine if a material is capable of thermochemical water-splitting, and, to good approximation, predict whether the thermodynamics are favorable for use under more challenging high-conversion conditions. This paper discusses the pros and cons of using TPTR and proposes a protocol for use within the STCH community.

Keywords: concentrated solar, thermogravimetry, screening, perovskite, water splitting, hydrogen Icroduction

OPEN ACCESS

Edited by:
Ellen B. Stechel,
Arizona State University, United States

Reviewed by:
Alicia Bayon,
Arizona State University, United States
Juan M. Coronado,
Institute of Catalysis and Petrochemistry (CSIC), Spain

***Correspondence:**
Ryan P. O'Hayre
rohayre@mines.edu

Specialty section:
This article was submitted to Hydrogen Storage and Production, a section of the journal Frontiers in Energy Research

Received: *17 January 2022*
Accepted: *08 March 2022*
Published: *08 April 2022*

Citation:
Sanders MD, Bergeson-Keller AM, Coker EN and O'Hayre RP (2022) A Thermogravimetric Temperature-Programmed Thermal Redox Protocol for Rapid Screening of Metal Oxides for Solar Thermochemical Hydrogen Production. Front. Energy Res. 10:856943. doi: 10.3389/fenrg.2022.856943

INTRODUCTION

Solar thermochemical water splitting (STCH) is an emerging technology that can be used to produce hydrogen gas from steam using thermal energy from the Sun *via* a two-step reduction and oxidation cycle (Bayon et al., 2020). While STCH has been shown to have theoretically high efficiencies (Steinfeld, 2005; Wang et al., 2012; Cheng et al., 2021), these values have yet to be attained in practice (Muhich et al., 2018), in part due to the thermodynamic limitations of the ceramic oxide materials used to perform the water splitting. The current state-of-the-art material for STCH is fluorite-structured ceria (CeO_2) (Lu et al., 2019), however perovskite oxides also hold much promise due to

their thermodynamic tunability, thermal and chemical stability over a wide range of temperatures and oxygen nonstoichiometries, and their compositional versatility (Scheffe and Steinfeld, 2014).

Many perovskite oxides have been explored in the context of STCH already (McDaniel et al., 2013; Barcellos et al., 2018), however benchmarking their performance relative to ceria is often a lengthy and unstandardized process. Efforts have been made to streamline the exploration of new STCH materials by comparing the oxygen vacancy formation energies (E_v) of prospective compounds relative to ceria [e.g., through thermodynamic computations using HSC (Abanades et al., 2006) and DFT (Emery et al., 2016; Bartel et al., 2019; Sai Gautam et al., 2020)] or by running thermochemical splitting experiments *via* thermogravimetry (TG) with CO_2 analogs (Nair and Abanades, 2018). However, these methods are often complex, time intensive and/or fall short of correctly predicting the water-splitting capability. Thus, it would be beneficial to the STCH community to find a new screening method that is relatively quick, simple, and provides sufficient information to reasonably predict a prospective material's water splitting potential. Here, we adopt a modified temperature-programmed reduction (TPR) methodology to quantify redox thermodynamics for this purpose.

TPR is most commonly associated with catalysis research (Hurst et al., 1982; Jones, 1986). In a typical TPR experiment, a sample is exposed to a flowing gas environment containing a reductant (hydrogen is the most prevalent) while the temperature of the sample is changed. The gas composition is monitored at the outlet of the reactor and the resulting changes in reductant concentration provide a "fingerprint" of the catalytic behavior. Other TPR implementations instead track changes in the mass of the sample being reduced or pressure changes in the reaction chamber.

In contrast to the general TPR approach described above, the TPR approach recommended for STCH materials discovery involves thermal rather than chemical reduction and incorporates a reoxidation step. To avoid confusion, it is therefore proposed that this technique be termed Temperature-programmed Thermal Redox (TPTR). TPTR offers significant benefits for STCH materials discovery as it is rapid (5.5 h per sample with only a few minutes of experiment setup) and it can be run on virtually any standard TG instrument without the need to add gas detection or advanced gas switching capabilities.

To illustrate the TPTR protocol, this study focuses on six candidate STCH compositions that span a broad range of possible STCH-relevant thermodynamic behavior. Three of the chosen compositions are perovskite structured manganates; $Sr_{0.95}Ce_{0.05}MnO_{3-\delta}$ (SCM05), $Sr_{0.9}Ca_{0.1}Ti_{0.7}Mn_{0.3}O_{3-\delta}$ (SCTM9173), and $Sr_{0.7}Ca_{0.3}Ti_{0.7}Mn_{0.3}O_{3-\delta}$ (SCTM7373). The two SCTM compositions were identified using the predicted performance from a STCH related Materials Project contribution (Vieten et al., 2019). Notably, the two end members STM and CTM were also later shown to be promising STCH candidates (Qian et al., 2020; Qian et al., 2021). In contrast, SCM05 was originally part of a broader study of the water-splitting SCM family (Bergeson-Keller et al., 2022), but it was predicted to have poor water splitting performance compared to higher Ce-content SCM compositions. In addition to the three manganates, two barium niobium ferrites, the double-perovskites $Ba_2FeNbO_{6-\delta}$ (BFN), and $Ba_2Ca_{0.66}Nb_{0.68}Fe_{0.66}O_{6-\delta}$ (BCNF), were selected due to the former's photocatalysis and CO_2 reduction potential (Voorhoeve et al., 1974; Zhang et al., 2017). Finally, CeO_2 (ceria) was included as a known state-of-the-art STCH material (Chueh et al., 2010) for comparison.

All compositions were screened using TPTR and the results analyzed using several different normalizations. The materials were also tested using an actual water-splitting test-stand to evaluate their water-splitting performance. The results from the two techniques were used to define target windows for the proposed figures of merit. This work will show that TPTR can accurately predict the water-splitting performance of new materials without the need for large sample quantities or specialized equipment.

EXPERIMENTAL

Powder Synthesis and Characterization

Powders used for this study were synthesized except for CeO_2, which was purchased (99.99% purity). SCM05 was synthesized *via* the sol-gel modified Pechini method described in detail elsewhere (Shang et al., 2013). Briefly, stoichiometric amounts of transition metal nitrates were weighted and dissolved in aqueous solution. Citric acid and Ethylenediaminetetraacetic acid (EDTA) were added to the solution as complexing agents in ratios of 3:1 to the metal cations. The reactants were dissolved in deionized water and ammonium hydroxide to achieve a pH close to 9, then the solution was heated to 350°C and stirred continuously until it became gelatinous. Finally, the gel was dried in a furnace held at 125°C overnight and calcined in air at 800°C for 10 h, then at 1,400°C for 5 h using a ramp rate of 5°C/min, and ground into a fine powder using a mortar and pestle.

The other compositions were synthesized using a solid-state reaction method. Briefly, stoichiometric amounts of various carbonates and oxides were mixed and dry planetary milled for 24 h then dried in air on a hot plate. The two SCTM compositions were pressed into pellets before calcination in air (500°C for 1 h, then 1,300°C for 12 h). The ferrites were directly pre-calcined (1,000°C for 10 h) before being wet planetary milled for 12 h then pressed into a pellet and calcined at 1,400°C for 10 h.

Powder X-ray diffraction (XRD) was conducted using Cu-Kα radiation (PANalytical/X'Pert PRO MPD, λ = 1.5406 Å, 2θ = 20–120°, 0.016 s^{-1} scan rate, 45 kV/40 mA output) and the target phases were confirmed *via* Rietveld refinement using Fullprof software.

TPTR

Overview of Necessary Equipment

In general, almost any TG is capable of TPTR. If the furnace has a suitable maximum temperature (>1,300°C for reasonable results) and the reactor chamber can be purged of oxygen to at least an oxygen partial pressure of 1 mbar (although lower than 0.001 mbar

is preferred), most of the TPTR protocol can be followed. Realtime oxygen sensing, either with a mass spectrometer or an oxygen sensor is helpful, especially for quantifying the actual reaction chamber pO_2, but this is not required. To fully carry out the experimental protocol, the TG should also be capable of changing gas environments while at temperature: specifically, flowing oxidizing gasses at temperatures of <1,000°C[1]. Most commercial TG balances have adequate resolution for TPTR as the experiments are designed to push the sample to high levels of oxygen non-stoichiometry. For instruments that have lower sensitivities, increased sample masses can often overcome this limitation (this and other sample considerations are discussed in more detail below). Unlike experiments designed to accurately capture the thermodynamics of reduction, TPTR is not as concerned with lower temperature non-stoichiometry behavior. For this reason, the need to control the chamber pressure using a back-pressure regulator is less important. Such regulation is far more important for long duration tests (tens of hours or days) and small mass losses (<100 μg).

Experimental Sample Considerations

Best results come from powder samples that have already experienced temperatures at least as high as those of the T_{red} step. This requirement is typically satisfied by the calcination procedure used during synthesis. This thermal stability requirement acts as an initial screen in case the composition cannot survive the temperatures used in the TPTR test (either due to decomposition, metal volatilization, or even melting). Particle size is not critically important, as long as the particles are <500 μm. Fine particles, like those that result from sol-gel synthesis, will give results closer to equilibrium, but in deeper powder beds, a fine powder size can lead to unreliable results due to gas diffusion effects. Sintering can also occur when using small powder sizes, although typically this has a relatively minor effect on the results.

Typical Experimental Conditions and Considerations

The TPTR experiments discussed in this study were conducted using a Setaram TGA (Setsys Evolution). Between 50 and 75 mg of sample powder was loaded into a platinum or alumina crucible. An initial oxygen burnout/reoxidation was performed in air up to 800°C and then the sample was cooled. The TPTR run begins with a ramp at 20°C min^{-1} to 1,350°C with a soak for 1 h in Ultra High Purity (UHP) N_2 at a flow rate of 100 sccm while the mass change due to thermal reduction is continuously monitored. The sample is then cooled at 20°C min^{-1} to 1,000°C and air is subsequently introduced for another hour to measure the reoxidation behavior, before finally cooling to 25°C at 10°C min^{-1}. Buoyancy effects are subtracted using a blank run of dense alumina balls of similar volume as the powder sample. Temperatures for the reduction and oxidation steps should be chosen based on the type of STCH cycle that is being investigated—here 1,350 and 1,000°C respectively, although higher or lower temperatures can also be examined. Many of the other parameters are chosen for convenience and can be adjusted with some consideration.

The optimal mass of sample is typically dictated by crucible volume, bed depth, and balance sensitivity. In principle, researchers should aim to use a sample mass and crucible configuration that produces a total mass loss two orders of magnitude larger than the noise floor of the instrument while yielding the shallowest possible bed depth to minimize gas diffusion effects. Higher signal-to-noise ratios are preferable, but not required. Exceptionally large amounts of sample can negatively impact test results. If powder beds are too deep, evolved oxygen may have trouble diffusing out of the bed, thereby elevating the local oxygen partial pressure and suppressing reduction. Even if the oxygen can escape the local sample area, if it cannot be properly swept out of the reaction chamber, oxygen build-up can again suppress reduction—thus the total volume of sample relative to the volume of the reaction chamber and the sweep-gas volumetric flow rate is also an important consideration.

The concerns discussed above motivate careful consideration of the impact of gas flow rates and heating rates. While low flow rates can assist in creating better TG traces, if the rate is too low, oxygen can accumulate in the chamber as mentioned above. Similarly, heating rates that are too fast can introduce a temperature lag into the sample (the reported temperature of the sample is not the actual temperature due to thermal diffusivity effects) and may also not allow enough time to sweep away evolved oxygen.

Because of the above considerations, it is recommended to run a couple of known samples under various experimental conditions to ensure that all necessary behavior is being captured. Ceria is a good choice to ensure that sample masses are adequate to capture low-reduction behavior. A few runs with decreasing amounts of sample can be used to identify when the mass loss can no longer be reliably measured. Most perovskites, especially an easily reduced compound like SCM05, will likely expel enough oxygen during reduction to affect the local oxygen partial pressure. A few experiments subjecting a known, easily-reduced STCH oxide (e.g., SCM05 or $Sr_aLa_{1-a}Mn_bAl_{1-b}O_{3-\delta}$) to increasing flow rates of gas can be used to identify a sufficiently high flow rate such that the amount of reduction remains constant from run to run, thereby ensuring that oxygen accumulation is not impacting results.

Water-Splitting Tests

Sandia National Laboratories' stagnation flow reactor (SFR) was used for water-splitting performance testing. The reactor employs a laser-based sample heater and utilizes a mass spectrometer downstream from the reactor to measure evolved gases (minus water). The details of the system have been published elsewhere (Scheffe et al., 2011; McDaniel et al., 2013). Briefly, approximately 100 mg of each of the powder samples are placed on a zirconia platform forming a loosely-packed shallow bed, and the reactor is heated to an oxidation temperature (T_{ox}) of either 850°C or 1,000°C

[1]It is possible to run the reduction and oxidation segments non-sequentially, with a cool down in between, but the oxidation will then occur at a less than optimal temperature, complicating the analysis. This also requires that the reduced state be thermally quenched in the low p_{O2} environment. A slow cooling rate allows the sample to getter oxygen from the gas environment, creating additional analysis complications.

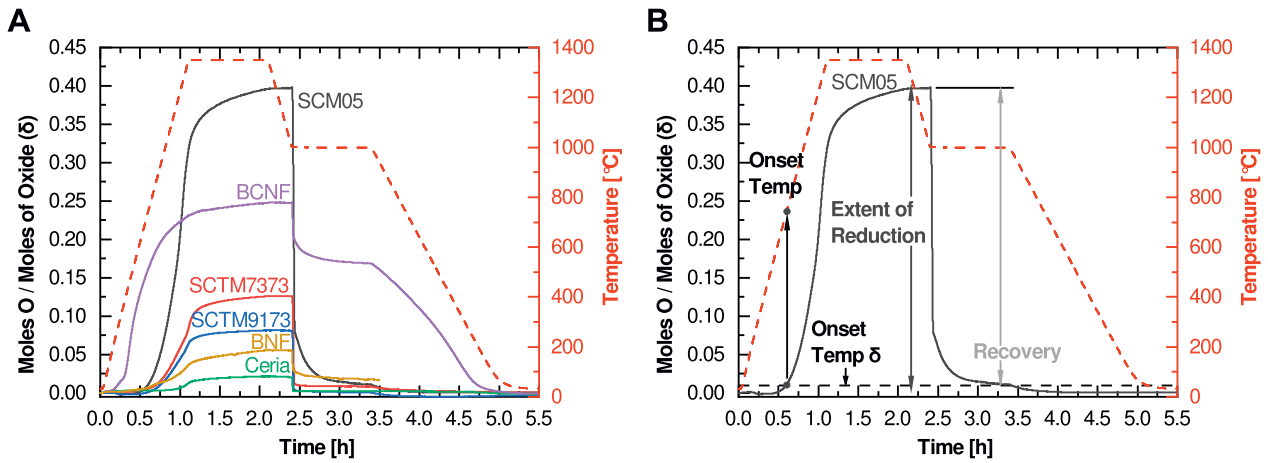

FIGURE 1 | (A) TPTR results for the six compositions of interest. **(B)** Visual descriptions of the three figures of merit for SCM05.

under UHP Ar atmosphere. Samples are heated by the laser at a controlled rate of 10°C/s from T_{ox} to a reduction temperature (T_{red}) of either 1,350°C or 1,400°C, where they are held for 330 s. Upon turning off the laser, the samples cool to T_{ox} in a matter of seconds, minimizing the potential for reoxidation with any trace amount of O_2 still in the chamber. 40 vol% water vapor in Ar gas flow is introduced to the system to initiate reoxidation. Reoxidation is conducted for 1,200 s. The total amount of H_2 produced is calculated by integrating the baseline-corrected mass spectrometer signal over the entire gas evolution envelope. Two additional redox cycles are then executed without a complete reoxidation in air.

RESULTS AND DISCUSSION

The TPTR results for the six compositions in this study are shown in **Figure 1**. The original mass traces were converted and normalized to δ using **Eq. 1**:

$$\delta = -\left(\frac{\Delta m}{M_O}\right)\left(\frac{M_{oxide}}{m_{oxide}}\right) \equiv \frac{\text{Moles O}}{\text{Moles Oxide}} \quad (1)$$

where Δm is the mass change, m_{oxide} is the initial mass of sample oxide, and M_{oxide} and M_O are the molar mass of the oxide and atomic oxygen, respectively. The sign is reversed so that positive values signify increases in δ. Other normalizations can be used, as discussed later. Rather than relying on qualitative evaluation to make determinations on STCH suitability, we advocate quantitative analysis of the TPTR results using three calculable figures of merit. An in-depth example illustrating the calculation and interpretation of these three figures of merit is provided in following sections.

Figures of Merit

Onset Temperature

The first proposed metric is the reduction onset temperature. The onset temperature is a construction borrowed from other thermal analysis techniques that investigate thermally activated reactions and processes. However, since reduction is a continuous thermal process (there is no sharp and distinct temperature onset for reduction in contrast to melting or solid-state phase changes), we consider here a modified application of the concept. Rather than attempting to determine the temperature at which the first measurable reduction occurs, we suggest using the temperature at which the extent of reduction reaches 0.01 (**Figure 2A**), or in cases where the room temperature non-stoichiometry is non-zero, when the thermal reduction component reaches 0.01. The onset temperature is closely correlated with the enthalpy of reduction (related to the formation enthalpy of oxygen vacancies), so higher reduction enthalpies should correspond to higher onset temperatures.

For the compositions investigated here, only two had an onset temperature below 800°C (BCNF and SCM05). Most high-potential water splitting materials exhibit reduction onset temperatures of at least 800°C, although as will be seen later there are examples of active water-splitting materials with reduction onset temperatures as low as 625°C. Thus, the reduction onset temperature metric cannot be used in isolation to evaluate water splitting potential. At the other end of the spectrum, ceria's onset temperature of 1,300°C is consistent with its nonviability for cycles designed around lower reduction temperatures. Favorable reduction onset temperatures between 800 and 1,000°C are observed for the remaining three compositions (SCTM7373, SCTM9173, and BNF).

Extent of Reduction

The second proposed figure of merit focuses on the total extent of reduction at the temperature of interest (in the investigations illustrated here, that is a T_{red} of 1,350°C). It is best evaluated at the end of the high temperature reduction soak (**Figure 2B**). This metric is more straightforward and intuitive than reduction onset temperature. It captures the degree of non-stoichiometry achieved for a given material at the given T_{red}. If evaluated as a function of soak-time, it can also provide some insight into the kinetics of the reduction process, although due to the many

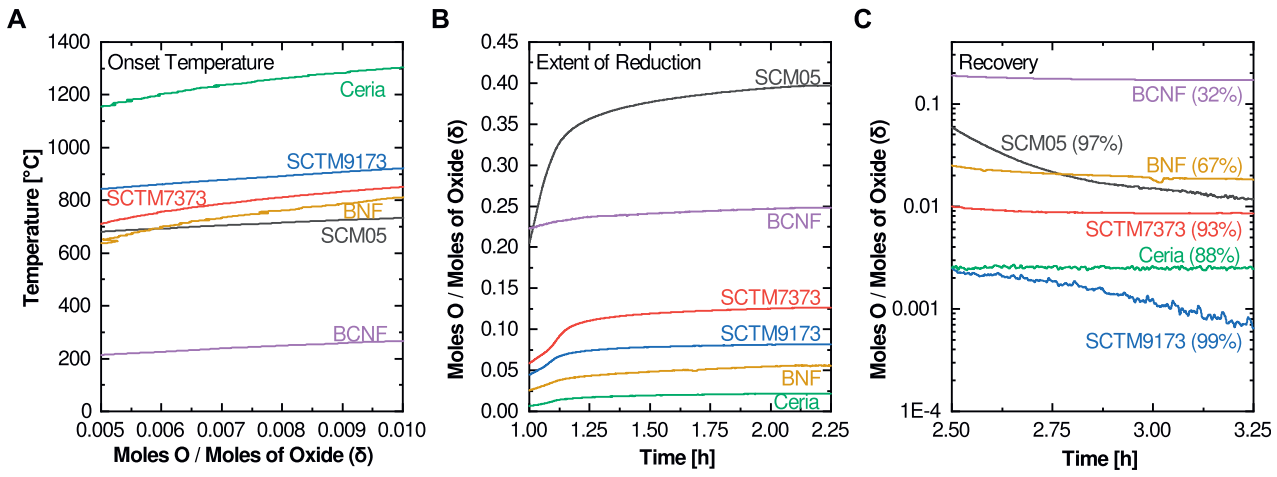

FIGURE 2 | Highlight plots of the relevant experimental data regions for the three figures of merit: **(A)** Onset Temperature, **(B)** Extent of Reduction, and **(C)** Recovery (calculated percentage of reoxidation at 1,000°C is also listed).

variables that influence kinetics, both from a material and experimental standpoint, kinetics is not considered in this screening method. In most cases, the optimal target for this metric is rapid equilibration to a moderate level of reduction. Higher levels of reduction typically signify that the material is too easily reduced and thus it is unlikely to reoxidize under water-splitting conditions. Low extents of reduction mean that the per-cycle hydrogen yield is likely to be too low for viability. This is examined in more detail later.

Ceria and BNF have extent of reduction values that are likely too low for viable water splitting potential, while the extent of reduction value for SCM05 is likely too high. Although BCNF has an attractive extent of reduction, its extremely low reduction onset temperature suggests that it is not a viable candidate. This again leaves the SCTM compositions as the most favorable candidates.

Recovery

The final figure of merit concerns the reoxidation behavior. Because reoxidation occurs in air rather than steam in this protocol, the reoxidation metric does not provide direct insight into the oxidation behavior of a material under actual water-splitting conditions. The potential to split water is best evaluated using the first two metrics, which more closely correspond to the thermodynamic potential for water splitting. Thus, this reoxidation metric, which we term "recovery", is instead best used to provide insight into the cyclability and stability of a candidate material. Like extent of reduction, this metric is best evaluated after the high-temperature reoxidation soak (**Figure 2C**) and can either be evaluated as the δ value or as a percentage of the extent of reduction. A perfect result is a return to the zero δ or zero Δδ condition (or 100% recovery). In some cases, this value will be either greater or less than the extent of reduction, in which case a secondary metric at room temperature can be informational. If the mass returns to the initial value only upon fully cooling to room temperature, this implies that full reoxidation cannot occur at T_{ox} even with air as an oxidant;

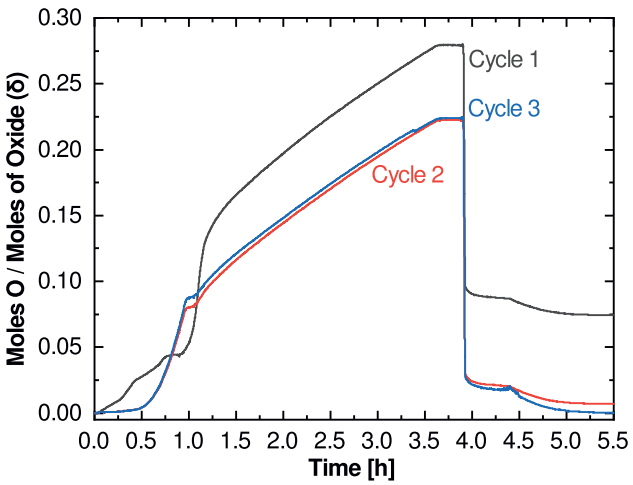

FIGURE 3 | Cycles of TPTR in BCM (Barcellos et al., 2018). adapted and used by permission of The Royal Society of Chemistry.

reoxidation in steam will therefore likely be greatly limited, and thus per cycle hydrogen production will be low or non-existent. If the material does not fully reoxidize even after reaching room temperature, the material is likely either unstable or has undergone an irreversible phase change. This is seen in the case of $BaCe_{0.25}Mn_{0.75}O_3$ (BCM) (**Figure 3**): an initial phase change leads to an incomplete reoxidation during the first measurement cycle, however, subsequent cycles do not show the same behavior as the material retains its new phase and the redox behavior stabilizes.

Considering the 6 materials tested here, BCNF shows poor recovery with a final value of ~0.18. When compared against its extent of reduction value of ~0.25, this gives a relative recovery of only 32%, strongly reinforcing the conclusion that BCNF is a nonviable candidate for STCH application. Similarly, the 67% recovery metric determined for BNF, when taken in concert with its low extent of reduction, suggests it is also not likely to be a

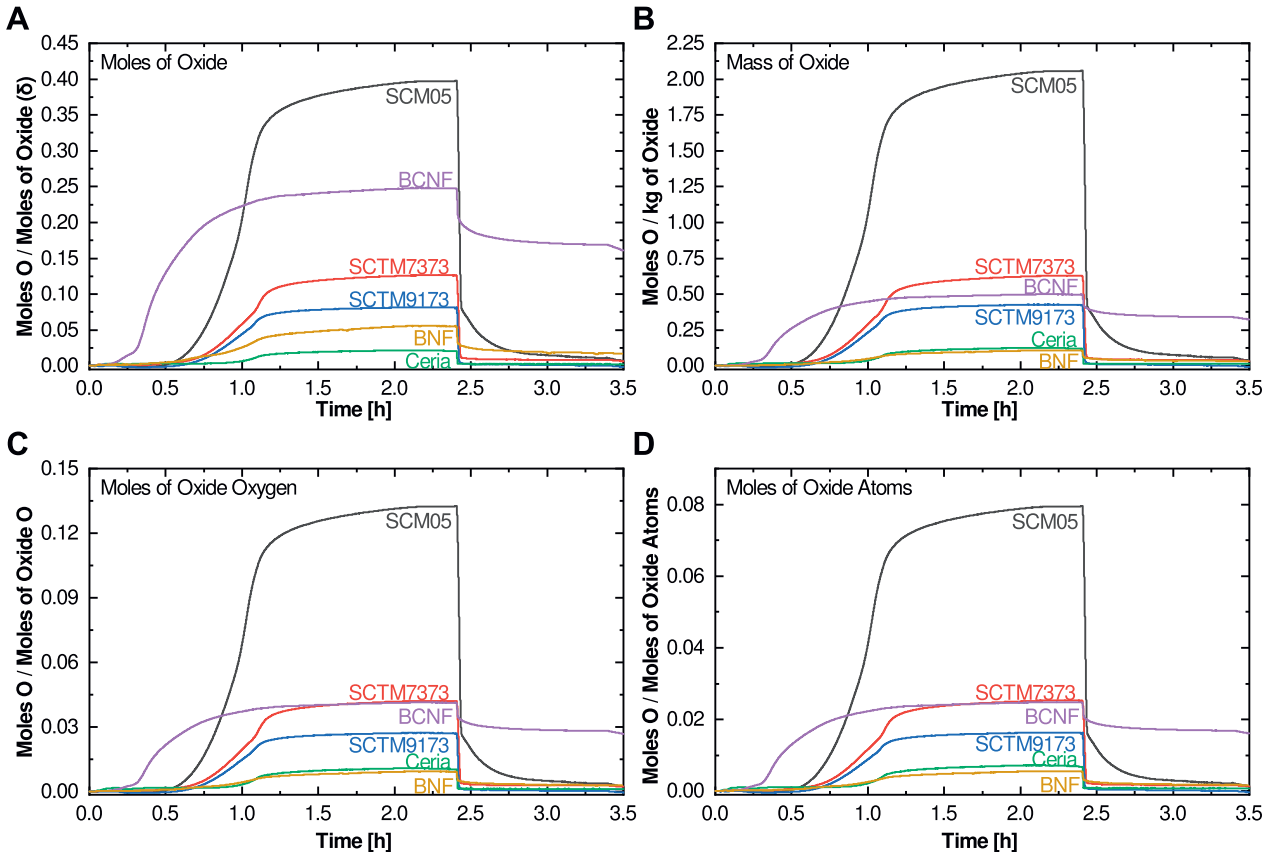

FIGURE 4 | Plots of four different normalization of the TGA data from the TPTR experiments: namely normalization by **(A)** moles of oxide, **(B)** mass of oxide, **(C)** moles of oxide oxygen, and **(D)** moles of oxide atoms.

promising water splitting candidate. In contrast, SCTM9173 nearly reaches 100% recovery, suggesting that it is therefore very likely to split water and maintain stability during cycling. Finally, SCM05 and SCTM7373 yield recovery values of 98 and 93%, suggesting that they also show promising cyclability and may provide sufficient reoxidation potential under water splitting conditions for continued consideration. Ceria's seemingly low 88% recovery is more a function of the low extent of reduction and resulting measurement uncertainty. The final δ of 0.002 is low enough to be essentially zero and can be considered 100% recovery.

Examining Alternative Normalizations

The TPTR trace analyses discussed so far are based on a normalization of the moles of oxygen released per mole of sample oxide. This is convenient since it is equivalent to δ, but there are potential issues with this normalization approach. Built into this normalization is a bias against compositions with less oxygen per formula unit (e.g., ceria's two oxygens vs. BCNF's six). Alternative options for normalization can shift the results of the figures of merit (mostly extent of reduction, the others are largely unaffected), potentially enabling a more representative analysis. **Figure 4** compares four different normalization options; namely normalization by (A) moles of oxide, (B) mass of oxide, (C) moles of oxide oxygen, and (D) moles of oxide atoms. Oxide mass normalization (**Figure 4B**) leads to dramatic shifts in the BNF and BCNF traces, while the others are only modestly affected. The shifts between **Figures 4A,B** are simply due to the way the chemical formulae for the double perovskites are written (or how the unit cell is defined) and do not reflect any fundamental changes in materials behavior. For mass-based normalization, there will also be a bias towards lighter elements, although this does not appear to be a large driver in STCH viability. It is possible to remove both the formula and mass bias by normalizing with a metric that better captures the relative oxygen content of each material. One possibility is to normalize by the number of moles of oxygen in the oxide. This normalizes differences between simple oxides like ceria and complex oxides like BCNF and BNF. As shown in **Figure 4C**, this normalization procedure results in additional shifts for BCNF and BNF. Most of the other compositions remain unchanged since they are simple perovskites. Finally, as shown in **Figure 4D**, the normalization can be taken one step further so that all the atoms in the oxide, rather than just the oxygen atoms are used in the normalization. This makes a small difference for the simple fluoride ceria, but most other compositions remain unaffected compared to normalization by the oxygen-atoms only.

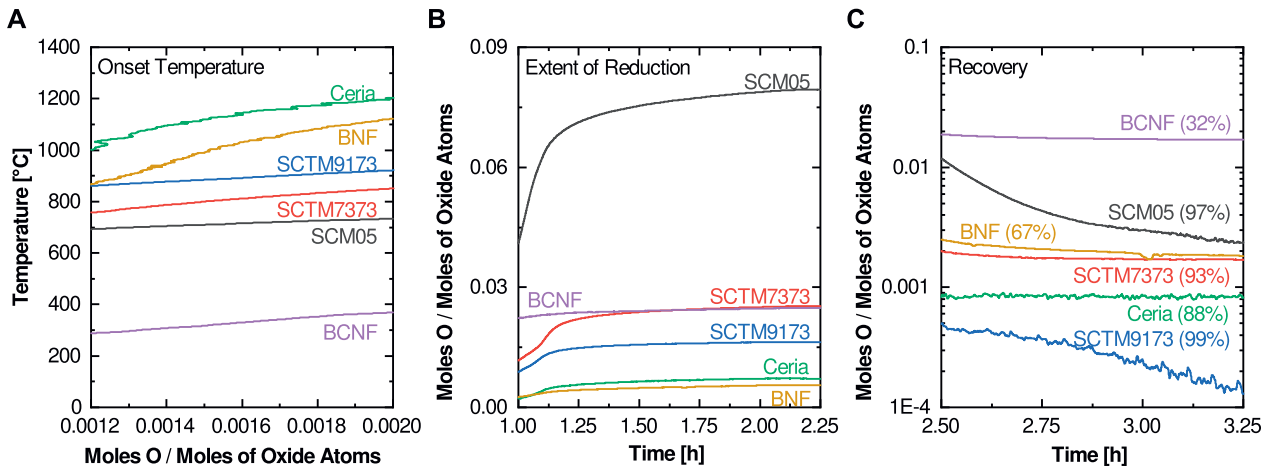

FIGURE 5 | Highlight plots of the relevant experimental data regions for the three figures of merit after re-normalization using moles of oxide atoms: **(A)** Onset temperature, **(B)** Extent of reduction, and **(C)** Recovery (calculated percentage of reoxidation at 1,000°C is also listed).

Importantly, however, the total number of atoms has a strong influence on the heat capacity of a material, which unlike mass alone, is strongly correlated with STCH efficiency. For that reason, total atoms is increasingly viewed as the preferred normalization for hydrogen productivity, so we propose employing this normalization option (i.e., **Figure 4D**) for TPTR analysis as well.

Revisiting the figures of merit to account for the moles of oxide atoms normalization approach (**Figure 5**) shows that, with the exception of BNF, the order for onset temperature and recovery for the six oxides examined here do not change relative to the original normalization approach (although as expected, the actual magnitudes have changed such that target ranges need to be revised). The exception is the large increase in onset temperature for BNF. This is most likely an artifact of the dramatic change in slope of the low temperature portion of the curve between the two normalizations. BCNF and BNF show dramatic changes in the extent of reduction using the moles of oxide atoms normalization approach; under this normalization method, BCNF is seen to be a more attractive candidate than previously viewed, although its other figures of merit remain poor. Even with the modified normalization, BNF does not appear to be viable for STCH application.

Correlation With Water-Splitting Performance

Five of the new compositions were sent to Sandia National Lab for water-splitting experiments using their SFR (SCM05 was estimated from data for higher ceria contents published in Bergeson-Keller et al.). By comparing the TPTR screening results to the SFR water splitting results, we identified target ranges for the three figures of merit that result in water splitting activity. **Figure 6** plots a wide variety of compositions, both those obtained directly from this study as well as results from other relevant published materials, using the first two figures of merit as the coordinate axes (**Figure 6A** uses the simple normalization while **Figure 6B** uses the number of oxide atoms normalization). **Table 1** summarizes all included materials and their hydrogen yields.

The results show that low onset temperatures and high extents of reduction are indeed strongly associated with little or no water splitting. While there doesn't appear to be a strong correlation between the hydrogen yields and position on either axis, there is nevertheless a clear clustering of the viable water-splitting materials. The cluster is tighter in **Figure 6A**, however the normalization in **Figure 6B** better predicts that BNF will behave like ceria. The shaded regions in **Figure 6** encompass most of the materials that successfully split water, and thus can be used to establish target ranges for reduction onset temperature and extent of reduction.

What is not captured in this representation is how the production will change under more challenging oxidation conditions. As discussed elsewhere (Bayon et al., 2022; Li et al., 2022), there is a problem with most perovskite compositions as an excessive quantity of steam is needed to produce significant hydrogen. In most cases, steam-to-hydrogen ratios in excess of 500:1 are necessary for compositions like SLMA to split at all. This inefficiency has hindered the adoption of perovskites as viable STCH materials. Testing under ratios lower than pure steam has only been carried out for select materials in this study and a few others. As the results show in **Table 1**, only ceria and BCM continue to split water near the levels achieved under pure steam, all other drop to less than 32%. Interestingly, ceria and BCM lie at different ends of the target window. BCM may be an outlier, however, since most analysis strongly correlates higher reduction enthalpy values to improved performance under low steam-to-hydrogen ratio conditions (Muhich et al., 2018), which is also related to onset temperatures and extents of reduction closer to ceria than BCM (lower right corner of **Figure 6**).

Limitations and Pitfalls of TPTR

While TPTR is especially useful as a rapid screening method, it is not recommended as a replacement for actual thermochemical

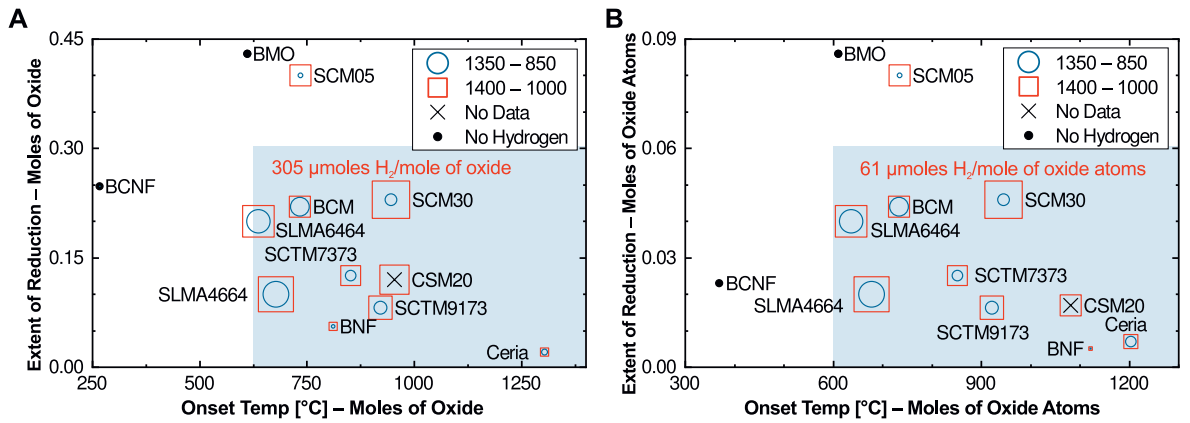

FIGURE 6 | Comparison of water-splitting hydrogen yields for new compositions, along with other published results from same facility, using both normalizations; **(A)** moles of oxide, and **(B)** moles of oxide atoms. Symbol sizes represent the magnitude of hydrogen produced during actual water-splitting for two different redox temperature pairs. The maximum production, SCM30 under the higher temperature conditions, is listed on the plot for scale. Shading indicates the target window for onset temperature and extent of reduction (McDaniel et al., 2013; Barcellos et al., 2018; Barcellos et al., 2019; Bergeson-Keller et al., 2022).

TABLE 1 | Summary of hydrogen yields from water-splitting experiments.

	μmoles H_2 per Mole of Oxide		μmoles H_2 per Mole of Oxide Atoms		% Of Max H_2 Production at H_2O:H_2 Ratio of 1,333:1
	1,350–850	1,400–1,000	1,350–850	1,400–1,000	
Ceria	51	71	17	24	100[c]
SCM05[b]	40[a]	175[a]	8[a]	35[a]	—
SCTM9173	102	193	20.4	38.6	25
SCTM7373	83	166	16.6	33.2	—
BNF	32.4	78.4	3.2	7.8	32
BCNF	8.82	6.19	0.88	0.62	—
$Sr_{0.7}Ce_{0.3}MnO_{3-\delta}$ (SCM30)[b]	91	305	18.2	61	—
$BaMnO_{3-\delta}$ (BMO)[c]	0	0	0	0	—
$BaCe_{0.25}Mn_{0.75}O_{3-\delta}$ (BCM)[c]	140	181	28	36.2	71[c]
$Ce_{0.2}Sr_{1.8}MnO_{4-\delta}$ (CSM20)[d]	—	247	—	35	26
$Sr_{0.6}La_{0.4}Mn_{0.6}Al_{0.4}O_{3-\delta}$ (SLMA6464)[e]	175	263	35	53	—
$Sr_{0.4}La_{0.6}Mn_{0.4}Al_{0.6}O_{3-\delta}$ (SLMA4664)[e]	194	292	38	58.4	26[c]

[a]*Estimated.*
[b]*(Bergeson-Keller, Sanders, and O'Hayre 2022).*
[c]*(Barcellos et al., 2018).*
[d]*(Barcellos et al., 2019).*
[e]*(McDaniel et al., 2013).*

testing and/or thermodynamic studies. As stated previously, actual water-splitting capability correlates well with the TPTR predictions, but variations do occur, and two materials with similar TPTR results may nevertheless show significant differences in thermochemical activity and hydrogen production. We partly ascribe such discrepancies to a major limitation of TPTR: kinetic behavior is not fully captured. This is especially true for oxidation, where the use of air can mask problems in oxidation kinetics due to the larger required driving force and differing reaction mechanism(s) for reoxidation by water-splitting vs. simple reoxidation in air. Poor reduction kinetics can also mask true extent of reduction results. Another related limitation is that a full thermodynamic picture is not developed by the single set of conditions present in TPTR. Such testing is not meant to tease apart the enthalpic and entropic contributions for a given material, but rather give an indication as to whether such exploration is warranted.

Another limitation is that the TPTR screening test is most relevant to short, non-isothermal cycles. Materials designed for isothermal cycling or that rely on full phase changes would likely perform very poorly under these screening conditions. However, the basic premise of the TPTR screening procedure could be adapted by changing the experimental conditions to mimic isothermal redox cycling or use longer soak times to examine phase-change materials; it is possible that useful analogous figures of merit can be established for such scenarios.

Finally, one of the largest pitfalls of TPTR analysis, and non-stoichiometry analysis in general, is the complexity posed by multi-phase samples. If the sample of interest is not a single phase or undergoes decomposition into one or more new phases during the TPTR test, this can complicate or completely invalidate the screening results. The analysis is based on the implicit assumption that the entire sample behaves as a single redox-active phase. If a sample instead consists of an unknown mix of phases, each of which presents a different redox behavior, then the results require careful scrutiny. For example, if the redox active phase is a minority phase diluted by non-active secondary phases, the TPTR results will be skewed, especially the extent of reduction, which will be greatly underestimated. This may give false positives for compositions that would reduce too much if phase-pure or false negatives if the extent of reduction appears to be very low because only a small amount of redox active phase is present.

Equivalent Methods Using Other Experimental Techniques

A number of other experimental techniques can and have been used to produce similar evaluations of candidate STCH materials without resorting to direct water splitting tests. One alternative is to use a small plug flow reactor, preferably with a rapid heating furnace. Since the mass cannot be tracked in this case, the evolved gas is instead monitored to evaluate the amount of oxygen evolved during reduction and consumed during oxidation. This technique works best for evaluating the reduction process since the resulting sharp oxygen release signal peaks produced during reduction are easier to analyze than the low-signal sigmoidal curves produced by oxygen uptake during reoxidation. With additional complexity, a small solar simulator can be used to achieve similar reduction measurements (Charvin et al., 2007). While these and other techniques are capable of making analogous measurements of redox activity, our view is that they are generally more complex and/or require more specialized equipment than that needed for TPTR. Additionally, these alternative techniques often require far larger sample amounts than the <100 mg needed for TG screening.

CONCLUSION

Temperature-programmed thermal reduction (TPTR) provides a simple TGA-based single-run experiment that measures the redox behavior of a specimen under thermal reduction and reoxidation conditions relevant to STCH. As such, it provides valuable information that can be used to rapidly screen candidate STCH materials without the complexity associated with directly measuring water splitting performance. In this work, several unreported STCH candidates were screened using the TPTR technique, and their water-splitting potential was analyzed on the basis of three figures of merit: reduction onset temperature, extent of reduction, and reoxidation recovery. Target ranges for STCH viability were established by comparing the figures of merit to the actual measured water splitting behavior for a wide variety of materials. We hope that this demonstration motivates the community to consider TPTR as a standardized protocol for the exploration of new and promising STCH candidate oxide materials. For such consideration, a proposed protocol is given in the **Supplementary Material S1**.

DATA AVAILABILITY STATEMENT

The datasets presented in this study can be found in online repositories. The names of the repository/repositories and accession number(s) can be found below: https://datahub.h2awsm.org/.

AUTHOR CONTRIBUTIONS

MS contributed to design of the study and the development of the protocol and performed the bulk of experiments, as well as authored the manuscript. AB-K assisted with experiments and wrote sections of the manuscript. EC assisted with the protocol document. RO provided oversight and critical revisions. All authors contributed to manuscript revision, read, and approved the submitted version.

FUNDING

This material is based upon work supported by the US. Department of Energy's Office of Energy Efficiency and Renewable Energy (EERE) under the Hydrogen and Fuel Cell Technologies Office, Award Number DE-EE0008087 and as a part of HydroGEN Energy Materials Network (EMN) consortium. Sandia National Laboratories is a multi-mission laboratory managed and operated by National Technology and Engineering Solutions of Sandia, LLC, a wholly owned subsidiary of Honeywell International, Inc., for the US. Department of Energy's National Nuclear Security Administration under contract DE-NA0003525. The views expressed in the article do not necessarily represent the views of the DOE or the US. Government.

ACKNOWLEDGMENTS

The authors would like to thank everyone in the STCH community that has organized, assisted in running, and participated over the past 4 years in the HydroGen/AWSM Benchmarking and Protocols Workshops.

SUPPLEMENTARY MATERIAL

The Supplementary Material for this article can be found online at: https://www.frontiersin.org/articles/10.3389/fenrg.2022.856943/full#supplementary-material

REFERENCES

Abanades, S., Charvin, P., Flamant, G., and Neveu, P. (2006). Screening of Water-Splitting Thermochemical Cycles Potentially Attractive for Hydrogen Production by Concentrated Solar Energy. *Energy* 31 (14), 2805–2822. doi:10.1016/j.energy.2005.11.002

Barcellos, D. R., Sanders, M. D., Tong, J., McDaniel, A. H., and O'Hayre, R. P. (2018). BaCe0.25Mn0.75O3−δ-a Promising Perovskite-type Oxide for Solar Thermochemical Hydrogen Production. *Energ. Environ. Sci.* 11 (11), 3256–3265. doi:10.1039/C8EE01989D

Barcellos, D. R., Coury, F. G., Emery, A., Sanders, M., Tong, J., McDaniel, A., et al. (2019). Phase Identification of the Layered Perovskite CexSr2-xMnO4 and Application for Solar Thermochemical Water Splitting. *Inorg. Chem.* 58 (12), 7705–7714. doi:10.1021/acs.inorgchem.8b03487

Bartel, C. J., Rumptz, J. R., Weimer, A. W., Holder, A. M., and Musgrave, C. B. (2019). High-Throughput Equilibrium Analysis of Active Materials for Solar Thermochemical Ammonia Synthesis. *ACS Appl. Mater. Inter.* 11 (28), 24850–24858. doi:10.1021/acsami.9b01242

Bayon, A., de la Calle, A., GhoseGhose, K. K., Page, A., and McNaughton, R. (2020). Experimental, Computational and Thermodynamic Studies in Perovskites Metal Oxides for Thermochemical Fuel Production: A Review. *Int. J. Hydrogen Energ.* 45 (23), 12653–12679. doi:10.1016/j.ijhydene.2020.02.126

Bayon, A., de la Calle, A., Stechel, E. B., and Muhich, C. (2022). Operational Limits of Redox Metal Oxides Performing Thermochemical Water Splitting. *Energy Tech* 10 (1), 2100222. doi:10.1002/ente.202100222

Bergeson-Keller, A. M., Sanders, M. D., O'Hayre, R. P., and O'Hayre, R. P. (2022). Reduction Thermodynamics of Sr1− XCeXMnO3 and CeXSr2− XMnO4 Perovskites for Solar Thermochemical Hydrogen Production. *Energ. Tech* 10 (1), 2100515. doi:10.1002/ente.202100515

Charvin, P., Abanades, S., Flamant, G., and Lemort, F. (2007). Two-step Water Splitting Thermochemical Cycle Based on Iron Oxide Redox Pair for Solar Hydrogen Production. *Energy* 32 (7), 1124–1133. doi:10.1016/j.energy.2006.07.023

Cheng, W.-H., de la Calle, A., Atwater, H. A., Stechel, E. B., and Xiang, C. (2021). Hydrogen from Sunlight and Water: A Side-By-Side Comparison between Photoelectrochemical and Solar Thermochemical Water-Splitting. *ACS Energ. Lett.* 6 (9), 3096–3113. doi:10.1021/acsenergylett.1c00758

Chueh, W. C., Falter, C., Abbott, M., Scipio, D., Furler, P., Haile, S. M., et al. (2010). High-Flux Solar-Driven Thermochemical Dissociation of CO_2 and H_2O Using Nonstoichiometric Ceria. *Science* 330 (6012), 1797–1801. doi:10.1126/science.1197834

Emery, A. A., Saal, J. E., Kirklin, S., Hegde, V. I., and Wolverton, C. (2016). High-Throughput Computational Screening of Perovskites for Thermochemical Water Splitting Applications. *Chem. Mater.* 28 (16), 5621–5634. doi:10.1021/acs.chemmater.6b01182

Hurst, N. W., Gentry, S. J., Jones, A., and McNicol, B. D. (1982). Temperature Programmed Reduction. *Catal. Rev.* 24 (2), 233–309. doi:10.1080/03602458208079654

Jones, A. (1986). *Temperature-Programmed Reduction for Solid Materials Characterization*, New York: M. Dekker.

Li, S., Wheeler, V. M., Kumar, A., Venkataraman, M. B., Muhich, C. L., Hao, Y., et al. (2022). Thermodynamic Guiding Principles for Designing Nonstoichiometric Redox Materials for Solar Thermochemical Fuel Production: Ceria, Perovskites, and beyond. *Energ. Tech* 10 (1), 2000925. doi:10.1002/ente.202000925

Lu, Y., Zhu, L., Agrafiotis, C., Vieten, J., Roeb, M., and Sattler, C. (2019). Solar Fuels Production: Two-step Thermochemical Cycles with Cerium-Based Oxides. *Prog. Energ. Combust. Sci.* 75, 100785. doi:10.1016/j.pecs.2019.100785

McDaniel, A. H., Miller, E. C., Arifin, D., Ambrosini, A., Coker, E. N., O'Hayre, R., et al. (2013). Sr- and Mn-Doped LaAlO3−δ for Solar Thermochemical H2 and CO Production. *Energy Environ. Sci.* 6 (8), 2424–2428. doi:10.1039/C3EE41372A

Muhich, C. L., Blaser, S., Hoes, M. C., and Steinfeld, A. (2018). Comparing the Solar-To-Fuel Energy Conversion Efficiency of Ceria and Perovskite Based Thermochemical Redox Cycles for Splitting H_2O and CO_2. *Int. J. Hydrogen Energ.* 43 (41), 18814–18831. doi:10.1016/j.ijhydene.2018.08.137

Nair, M. M., and Abanades, S. (2018). Experimental Screening of Perovskite Oxides as Efficient Redox Materials for Solar Thermochemical CO_2 Conversion. *Sustain. Energ. Fuels* 2 (4), 843–854. doi:10.1039/C7SE00516D

Qian, X., He, J., Mastronardo, E., Baldassarri, B., Wolverton, C., Haile, S. M., et al. (2020). Favorable Redox Thermodynamics of SrTi0.5Mn0.5O3−δ in Solar Thermochemical Water Splitting. *Chem. Mater.* 32, 9335–9346. doi:10.1021/acs.chemmater.0c03278

Qian, X., He, J., Mastronardo, E., Baldassarri, B., Yuan, W., Wolverton, C., et al. (2021). Outstanding Properties and Performance of CaTi0.5Mn0.5O3-δ for Solar-Driven Thermochemical Hydrogen Production. *Matter* 4 (2), 688–708. doi:10.1016/j.matt.2020.11.016

Sai Gautam, G., Stechel, E. B., and Carter, E. A. (2020). Exploring Ca-Ce-M-O (M = 3d Transition Metal) Oxide Perovskites for Solar Thermochemical Applications. *Chem. Mater.* 32 (23), 9964–9982. doi:10.1021/acs.chemmater.0c02912

Scheffe, J. R., and Steinfeld, A. (2014). Oxygen Exchange Materials for Solar Thermochemical Splitting of H_2O and CO_2: a Review. *Mater. Today* 17 (7), 341–348. doi:10.1016/j.mattod.2014.04.025

Scheffe, J. R., Allendorf, M. D., Coker, E. N., Jacobs, B. W., McDaniel, A. H., and Weimer, A. W. (2011). Hydrogen Production via Chemical Looping Redox Cycles Using Atomic Layer Deposition-Synthesized Iron Oxide and Cobalt Ferrites. *Chem. Mater.* 23 (8), 2030–2038. doi:10.1021/cm103622e

Shang, M., Tong, J., and O'Hayre, R. (2013). A Novel Wet-Chemistry Method for the Synthesis of Multicomponent Nanoparticles: A Case Study of BaCe0.7Zr0.1Y0.1Yb0.1O3−δ. *Mater. Lett.* 92, 382–385. doi:10.1016/j.matlet.2012.11.038

Steinfeld, A. (2005). Solar Thermochemical Production of Hydrogen-Aa Review. *Solar Energy* 78 (5), 603–615. doi:10.1016/j.solener.2003.12.012

Vieten, J., Bulfin, B., Huck, P., Horton, M., Guban, D., Zhu, L., et al. (2019). Materials Design of Perovskite Solid Solutions for Thermochemical Applications. *Energ. Environ. Sci.* 12 (4), 1369–1384. doi:10.1039/C9EE00085B

Voorhoeve, R. J. H., Trimble, L. E., and Khattak, C. P. (1974). Exploration of Perovskite-like Catalysts: Ba2CoWO6 and Ba2FeNbO6 in NO Reduction and CO Oxidation. *Mater. Res. Bull.* 9 (5), 655–666. doi:10.1016/0025-5408(74)90136-6

Wang, Z., Roberts, R. R., Naterer, G. F., and Gabriel, K. S. (2012). Comparison of Thermochemical, Electrolytic, Photoelectrolytic and Photochemical Solar-To-Hydrogen Production Technologies. *Int. J. Hydrogen Energ.* 37 (21), 16287–16301. doi:10.1016/j.ijhydene.2012.03.057

Zhang, G., Sun, S., Jiang, W., Miao, X., Zhao, Z., Zhang, X., et al. (2017). A Novel Perovskite SrTiO3-Ba2FeNbO6Solid Solution for Visible Light Photocatalytic Hydrogen Production. *Adv. Energ. Mater.* 7 (2), 1600932. doi:10.1002/aenm.201600932

Conflict of Interest: The authors declare that the research was conducted in the absence of any commercial or financial relationships that could be construed as a potential conflict of interest.

The handling editor ES declared a past collaboration with the author(s) EC.